Quantum Electronics **46** (4) 315–320 (2016)

DOI: 10.1070/QEL16048

Nonlinear reflection of high-amplitude laser pulses from relativistic electron mirrors

V.V. Kulagin, V.N. Kornienko, V.A. Cherepenin

Abstract. **A coherent X-ray pulse of attosecond duration can be formed in the reflection of a counterpropagating laser pulse from a relativistic electron mirror. The reflection of a high-amplitude laser pulse from the relativistic electron mirror located in the field of an accelerating laser pulse is investigated by means of two-dimensional (2D) numerical simulation. It is shown that provided the amplitude of the counterpropagating laser pulse is several times greater than the amplitude of the accelerating laser pulse, the reflection process is highly nonlinear, which causes a significant change in the X-ray pulse shape and its shortening up to generation of quasi-unipolar pulses and single-cycle pulses. A physical mechanism responsible for this nonlinearity of the reflection process is explained, and the parameters of the reflected X-ray pulses are determined. It is shown that the duration of these pulses may constitute 50–60 as, while their amplitude may be sub-relativistic.**

Keywords: *generation of coherent attosecond X-ray pulses, ultraintense non-adiabatic laser pulses, relativistic electron mirrors.*

1. Introduction

Coherent attosecond pulses of X-ray and extreme ultraviolet range can find numerous applications in various fields of science and technology, particularly in biomedical research, spectroscopy, studies on the ultrafast structural dynamics of materials, etc. Elaboration of high-power femtosecond laser systems has stimulated the development of purely optical methods of generating such pulses. One of the most promising approaches is the use of reflection of counterpropagating laser pulses from a mirror moving at a relativistic velocity, since in this case, the frequency of the reflected pulse increases with decreasing its duration [1]. Furthermore, this system allows controlling not only the amplitude and frequency of the reflected pulse, but also its other parameters, in particular, the envelope shape, phase difference between the carrier and envelope, etc. As relativistic mirrors, use can be made of electron mirrors formed by high-power laser pulses from nanofilms [2, 3] or in gas jets [4], and also of plasma electron–ion mirrors formed by accelerating a target as a whole [5].

Lately, not only the processes of formation of relativistic electron mirrors from nanofilms and reflection of the counterpropagating probe pulses from these mirrors [2, 3, 6–15] have been theoretically studied, but also first experiments [16–18], which demonstrated the prospects of this approach, have been carried out. To form relativistic electron mirrors with parameters ensuring effective reflection of a counterpropagating probe pulse, stable freely suspended targets of nanometre thickness and high-power accelerating laser pulses with a steep enough leading edge and high contrast are required. Freely suspended carbon films with a thickness of 5 nm and more have been already relatively long used in physical experiments [19]. Recently, new methods for preparation of carbon nanofilms with required parameters [20, 21] have been actively developed. High contrast of an accelerating laser pulse is provided by means of plasma mirrors, which, as a result of plasma formation on the plasma mirror surface, transmit a fraction of the pulse with small amplitude and reflect its central part with maximum amplitude. This method of increasing the contrast is widely used in today's experiments with high-power laser installations and has demonstrated its efficiency in the use of targets from nanofilms [16–18, 22]. At the same time, the problem of forming an adiabatic laser pulse with a sufficiently steep leading edge has not yet been solved experimentally. However, theoretical studies show that a steep edge in a laser pulse can be formed by transmitting the pulse through an additional nanofilm [15, 23–26].

The nature of reflection of a counterpropagating laser pulse from a relativistic electron mirror depends on whether the mirror is located in the accelerating laser pulse or removed from it. The matter is that in reflection of the probe laser pulse with a relativistic amplitude from the mirror, electrons acquire an additional transverse momentum (along the mirror surface) associated with the probe pulse impact. If electrons have not possessed a transverse momentum before reflection, for example, have been removed from the accelerating laser pulse [12, 13], a significant slowdown of the mirror with a corresponding decrease in the reflected pulse frequency arises already in the case when the dimensionless probe pulse amplitude is on the order of unity. The dimensionless laser pulse amplitude has the form

$$a_0 = |e|E_0/(mc\omega), \tag{1}$$

V.V. Kulagin P.K. Sternberg Astronomical Institute, M.V. Lomonosov Moscow State University, Universitetskiy prosp. 13, 119991 Moscow, Russia; Institute of Radio Engineering and Electronics, Russian Academy of Sciences, ul. Mokhovaya 11, 125009 Moscow, Russia, e-mail: victorvkulagin@yandex.ru;
V.N. Kornienko, V.A. Cherepenin Institute of Radio Engineering and Electronics, Russian Academy of Sciences, ul. Mokhovaya 11, 125009 Moscow, Russia

Received: 24 February 2016
Kvantovaya Elektronika **46** (4) 315–320 (2016)
Translated by M.A. Monastyrskiy

where c is the speed of light in vacuum; ω and E_0 are the laser field frequency and amplitude in vacuum; and e and m are the charge and mass of an electron. In the case of a relativistic electron mirror located in the accelerating field of a laser pulse, electrons already have a transverse momentum defined by the accelerating field; therefore, no significant slowdown of the mirror occurs until the probe pulse amplitude becomes on the order of the accelerating pulse amplitude [15]. This provides good linearity of reflection, i.e. the reflection coefficient and the shape of the reflected pulse do not significantly change with increasing probe pulse amplitude from small values to a value having an order of the accelerating pulse amplitude. Theoretical estimates show that in this case, the dimensionless amplitude of the probe pulse of the order of square of the dimensionless amplitude of the accelerating pulse is required to stop the mirror [6].

The aim of this work is to study the reflection of high-amplitude probe laser pulses from relativistic electron mirrors located in the field of the accelerating laser pulse. It is shown that provided the amplitude of the counterpropagating laser pulse is several times greater than that of the accelerating laser pulse, the reflection process is highly nonlinear, which causes a significant change in the shape of the reflected X-ray pulse and its shortening down to generating quasi-unipolar pulses, with the amplitude of some half-cycle being several times greater than the amplitudes of other half-cycles, and also single-cycle pulses. The emergence of such nonlinearity is actually associated with the destruction of the relativistic electron mirror by the counterpropagating probe pulse. In addition, the large amplitude of the probe pulse leads to a significant curvature of the relativistic electron mirror, which determines the possibility of further focusing of the reflected X-ray pulse.

2. Changing the reflected pulses shape by increasing the probe laser pulse amplitude

A numerical code based on the 'particle-in-cell' method has been used for two-dimensional (2D) simulation. On the whole, the parameters of the accelerating pulse and the geometry of interaction correspond to those used in [15]. The accelerating non-adiabatic laser pulse propagates in the positive direction of the z axis and has a linear field polarisation along the x axis. The laser field wavelength in vacuum is $\lambda = 1$ μm, the beam diameter in the focus plane is 40λ at the e^{-1} level and the maximum amplitude of the dimensionless field is 10. The dependence of the accelerating pulse field E_x on the transverse coordinates and time is super-Gaussian (total duration is $6\lambda/c$ at the level e^{-1}), the initial phase being chosen in such a way that the amplitude of the first half-cycle is on the order of the maximum pulse amplitude [15]. To form the relativistic electron mirror, a nanofilm having a thickness of $l = 5$ nm at the electron density of $n_0 = 2.65\times10^{22}$ or 3.55×10^{22} cm^{-3} is used. The grid cell dimensions are $5.5\times10^{-4}\lambda$ along the z axis and $2\times10^{-2}\lambda$ along the x axis, each cell containing 70 particles (an increase in this parameter does not change the results of simulations).

In the experiment, solid-state nanofilms, the thickness of which is several times less, can be used [19–21]. However, numerical simulation of those nanofilms with a reduced thickness (and hence, with a higher electron density) is associated with a significant increase in the computational resources because of the need to reduce the cell size. At the same time, in the quasi-1D interaction regime, when the focal spot size is much larger and the film thickness is much smaller than the accelerating field wavelength, the dimensionless surface density of the target exerts a decisive effect on the nature of interaction [2, 3]

$$\alpha = \pi \frac{\omega_p^2}{\omega^2} \frac{l}{\lambda}, \qquad (2)$$

where $\omega_p = \sqrt{4\pi n_0 e^2/m}$ is the plasma frequency, which allows obtaining information on the behaviour of thin films by modelling the films with a larger thickness and a lesser electron density with preserving the α value. In our case, assuming that the actual target may have a thickness of 0.5 nm, we obtain its equivalent concentration $n_0 = 2.65\times10^{23}$ or 3.55×10^{23} cm^{-3}, which already corresponds to the solid-state concentrations. In the simulation, the nanofilm is assumed fully ionised (which is true for the field amplitudes used), and the plasma is collisionless. The ion mass m_i is taken equal to $1840m$. The ions remain virtually immobile at moderate α values within a short time of nanofilm electron acceleration. As a result, the acceleration process weakly depends on the content of the target, in particular, on the presence of heavy ions.

The shapes of the reflected pulse for different probe pulse amplitudes are shown in Fig. 1. The probe pulse propagates in the negative direction of the z axis, has linear polarisation along the y axis and Gaussian shape in space and time with a total duration of $2\lambda/c$ at the e^{-1} level, while in numerical simulation, its maximum dimensionless amplitude a_1 is varied in the range from 15 to 80 at the beam diameter equal to 16λ. The relativistic electron mirror is formed from a target with an initial electron concentration of $n_0 = 2.65\times10^{22}$ cm^{-3}. In the course of the probe pulse reflection, the relativistic electron mirror is located in the field of the accelerating pulse, while the interaction with the probe pulse begins three field periods after the acceleration starts.

For a minimal amplitude of $a_1 = 15$ (Fig. 1a), the reflected pulse corresponds in shape to the reflected pulses at small amplitudes of the probe pulse ($a_1 < a_0$), the reflected radiation wavelength varying from 12 nm at the pulse leading edge to 15 nm at the pulse trailing edge, which is explained by a slowdown of the relativistic electron mirror in the process of its interaction with the counterpropagating probe pulse. The total duration of the reflected pulse constitutes 130 as at the e^{-1} level; this interval comprises approximately three oscillation periods, while the probe pulse has two oscillation periods only, the thickness of the relativistic electron mirror at the moment of reflection of a part of the probe pulse with maximal amplitude being on average ~15 nm. Effective reflection of the probe pulse occurs as if it were from the boundaries of the relativistic electron mirror (similar to reflection from the semi-transparent mirror in conventional optics), the concentration near the left and right boundaries of the mirror being different, and therefore the coefficients of reflection from the boundaries being also different. The pulses reflected from different boundaries interfere, which explains an increase in the number of periods in the reflected pulse compared with the probe pulse. Thus, the absolute value of the reflection coefficient depends not only on the reflection moment (relativistic electron mirror is at the stage of acceleration, and its velocity increases), but also on the mirror thickness and electron density distribution within the mirror, which also change

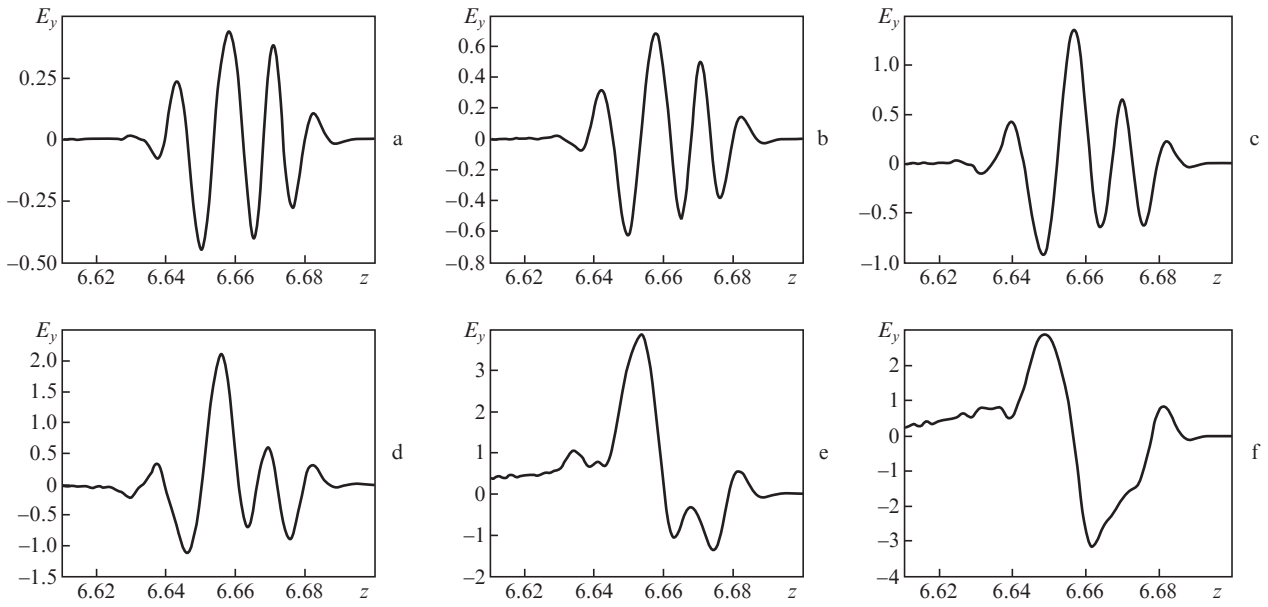

Figure 1. Field E_y of the reflected pulse on the axis of the beam propagating in the positive direction of the z axis. The maximum amplitude of the probe pulse is a_1 = (a) 15, (b) 20, (c) 30, (d) 40, (e) 60 and (f) 80. The accelerating pulse amplitude is $a_0 = 10$, the target thickness is 5 nm, the concentration of electrons is $n_0 = 2.65\times10^{22}$ cm^{-3}, and the relativistic electron mirror is located in the field of accelerating pulse. Here and in Figs 2, 3, the reflected field amplitude is normalised in accordance with expression (1), the laser radiation frequency being used for normalisation, and the coordinates being normalised by the laser radiation wavelength.

over time. The relativistic electron mirror boundaries in this case are rather sharp, i.e. the thickness of the layer, within which the electron density increases from zero to a maximum value, is much smaller than the wavelength of reflected radiation; as a result, the reflection efficiency turns out relatively high. The frequency change calculated by the longitudinal component of the relativistic electron mirror velocity is well-consistent with the wavelength of reflected radiation. For example, the frequency conversion coefficient for different mirror layers ranges between 80 and 91 before reflection of the probe pulse's half-cycles with maximum amplitudes, and between 55 and 68 after reflection. Similar reflection characteristics are on the whole valid for the probe pulse amplitude equal to 20, the reflected pulse amplitude being also increased (see Fig. 1). In particular, after reflection of the probe pulse's half-cycles with maximum amplitudes, the frequency conversion coefficient for different mirror layers ranges from 43 to 55.

A further increase in the probe pulse amplitude leads to significant changes in the reflected pulse shape. In this case, the first half-cycles of the probe pulse have insufficient amplitude for substantial deformation of the mirror; therefore, their reflection occurs according to the above-described scenario. In reflection of the probe pulse with maximum amplitudes of half-cycles, the longitudinal velocity of the mirror decreases and the reflection coefficient increases. This leads to an increase in the amplitudes of the half-cycles with maximum amplitudes compared with other half-cycles, i.e. the central part of the reflected pulse turns out efficiently 'pronounced' (Fig. 1c); moreover, in this case, the reflected pulse comprises two parts with different frequencies differing by 1.6 times. This effect is even more visible in Fig. 1d, where the amplitude of one of the reflected pulse's half-cycles reaches 2.15. With a further increase in the probe pulse amplitude, the mirror's slowdown significantly alters the phase relations for various half-cycles of the reflected pulse. At certain amplitude, the slowdown becomes so essential that the mirror 'transits' to other half-cycles of the accelerating pulse (Figs 1e and 1f). In this case, the reflected pulse frequency is reduced by several times, and the reflection is actually terminated. In this way, the quasi-unipolar pulses may be formed, with one half-cycle being several times larger in amplitude than the others (the positive half-cycle amplitude in Fig. 1e reaches 3.9 and by three times exceeds the amplitudes of other half-cycles, its duration constitutes about 65 as), or the pulses having one oscillation period (in Fig. 1f, the amplitude of the reflected pulse is equal to 3, the duration is about 130 as, which gives already a sub-relativistic intensity).

The field of the reflected pulse on the beam axis for the initial concentration $n_0 = 3.55\times10^{22}$ cm^{-3} and various probe pulse amplitudes is shown in Figs 2a–2c (other parameters of the target and also of laser and probe pulses are the same as in Fig. 1). Here, the initial concentration in the nanofilm is greater, and so the frequency conversion coefficient for small amplitudes of the probe pulse (Fig. 2a) turns out smaller than that in Fig. 1a [2, 3]; in other respects, the nature of variation of the reflected pulse shape is similar to that presented in Fig. 1. For example, the reflected pulse shown in Fig. 2c is quasi-unipolar (the large half-cycle duration is approximately 53 as; its amplitude is about 3.7). The unipolar pulses of attosecond duration with comparable parameters have also been obtained in numerical simulation of oblique incidence of a high-power laser pulse on a double-layer target consisting of two nanofilms located at a certain distance from each other [14]. Depending on the target and laser pulse parameters, our scheme allows the formation of coherent X-ray pulses of attosecond duration, containing one oscillation period or having a quasi-unipolar shape.

The maximum amplitude a_{max} of the reflected pulse and its ratio to the probe pulse amplitude $r_{max} = a_{max}/a_1$ for the fields represented in Figs 1 and 2 are shown in Fig. 3 as func-

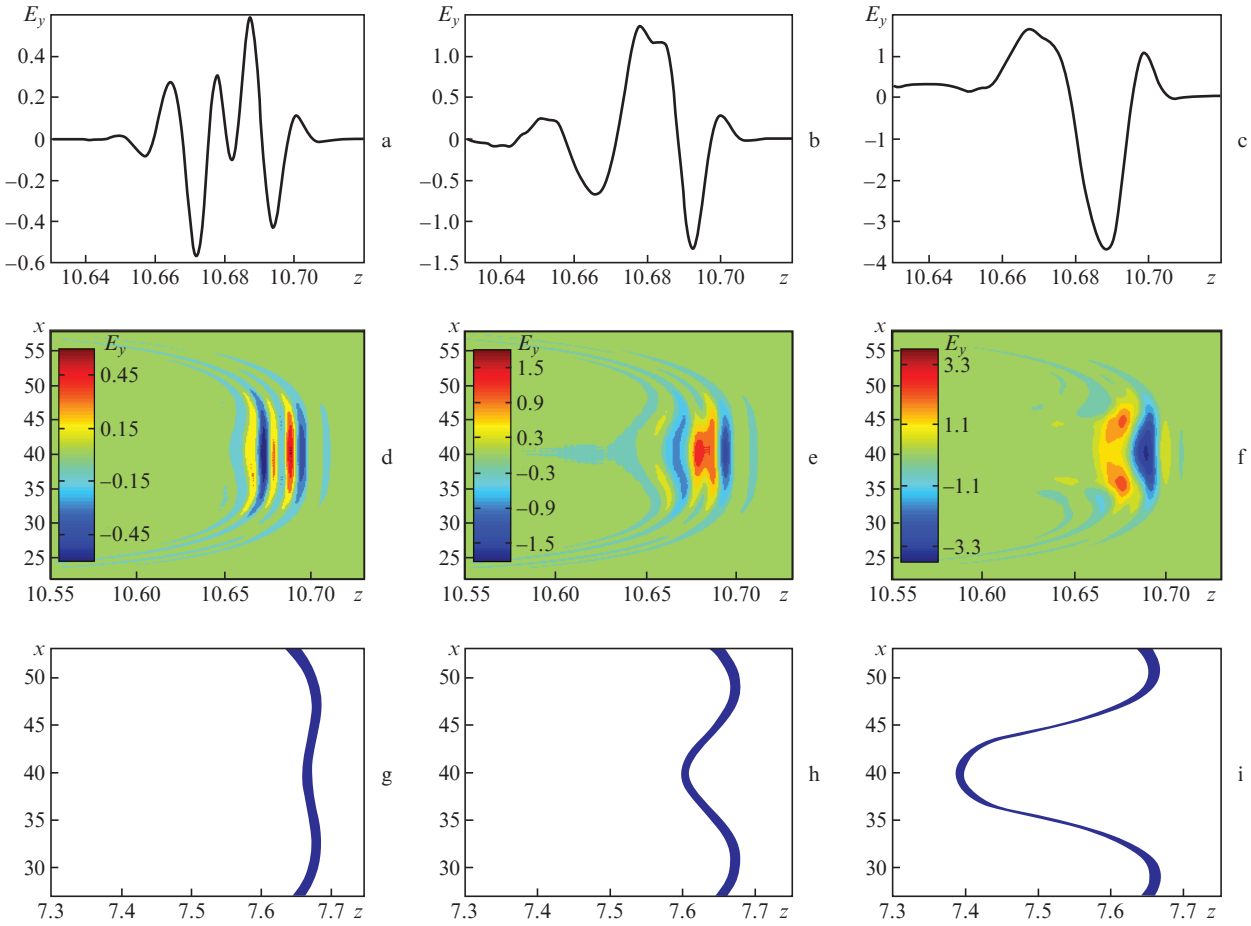

Figure 2. (Colour online) (a–c) Field E_y of the reflected pulse on the beam axis, (d–f) spatial structure of the reflected pulse and (g–i) shape of the relativistic electron mirror after reflection of a part of the probe pulse with maximum amplitudes of half-cycles. The maximum amplitude of the probe pulse is a_1 = (a, d, g) 20, (b, e, h) 40 and (c, f, i) 80. The concentration of electrons in the target is $n_0 = 3.55\times10^{22}$ cm^{-3}, other parameters are the same as in Fig. 1.

tions of the parameter a_1. The shape of the reflected pulse strongly changes with a_1, so that the values of a_{max} and r_{max} cannot, generally speaking, characterise the pulse reflection process as a whole. In simulation, the r_{max} value was about 3%–7%. A decrease in a_{max} and r_{max} with increasing a_1 from 60 to 80 for the nanofilm with an initial concentration of electrons 2.65×10^{22} cm^{-3} is probably explained by the fact that the reflected half-cycle with a maximal amplitude is formed in this case by a half-cycle that precedes the maximal half-cycle in the probe pulse (when the target thickness at the reflection moment is comparable with the wavelength of reflected radiation, more accurate matching of the half-cycles in the incident and reflected pulses is not possible).

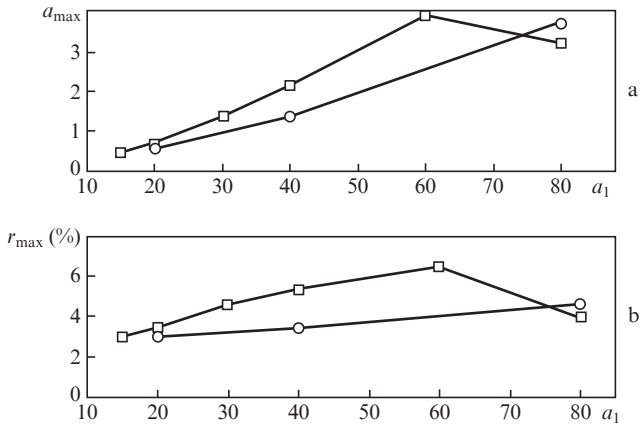

Figure 3. (a) Maximum amplitude a_{max} of the reflected pulse and (b) its ratio to the probe pulse amplitude $r_{max} = a_{max}/a_1$ as functions of a_1 at the initial electron concentration in the target $n_0 = 2.65\times10^{22}$ (□) and 3.55×10^{22} cm^{-3} (○).

3. Spatial structure of the reflected pulse and shape of the relativistic electron mirror

Spatial structure of the reflected pulse and shape of the relativistic electron mirror after reflection of a fraction of the probe pulse with maximum amplitudes of half-cycles are shown in Figs 2d–f and 2g–i. In the case that the probe pulse amplitude exceeds the accelerating pulse amplitude only twice (Fig. 2g), the sagging of the mirror after reflection of a part of the probe pulse with maximum amplitudes of half-cycles is about 12 nm, which is less than the wavelength of reflected radiation and much less than the wavelength of accelerating radiation. Thus, as Fig. 2d indicates, only the last two half-cycles of the reflected pulse have the corresponding

phase front curvature; the half-cycles in the leading part of the pulse have a virtually flat front. At the probe pulse amplitude $a_1 = 40$, the sagging of mirror turns out about 70 nm (see Fig. 2h), which is much larger than the reflected pulse wavelength, but considerably smaller than the accelerating pulse wavelength. The phase front deformation begins even before the arrival of the probe pulse with maximum amplitudes of half-cycles (Fig. 2e), a majority of the half-cycles of the reflected pulse have the curved phase fronts; however, the mirror is not destroyed at the end of reflection and continues to move as a whole, remaining on the same half-cycle of the accelerating pulse. Finally, at the amplitude $a_1 = 80$, only a fraction of the probe pulse up to the first half-cycle with a maximum amplitude is reflected; after this, the mirror velocity in its central part is significantly reduced, so that the frequency conversion coefficient turns out decreased to 10. After reflection of a fraction of the probe pulse with maximum amplitudes of half-cycles, the sagging of the mirror constitutes about a quarter of the laser wavelength, i.e. the middle part of the mirror moves to the next half-cycle of the accelerating pulse. At a later stage, the sagging of the mirror is even more increased and by the end of reflection reaches a value greater than two wavelengths, which means that the mirror turns out almost destroyed.

The wavefront curvature of the reflected pulse indicates a possibility of its focusing, and the curvature of the relativistic electron mirror can be changed by increasing or decreasing the probe pulse amplitude. This provides a way of controlling the position of the focal point of the reflected X-ray pulse. However, we should take into account that the wavefront curvature of the reflected pulse is sufficiently small (the scales on the x and z axes in Figs 2d–2f differ by 200 times). Simple estimates show that a distance of several millimetres is required for focusing of such a pulse (about 3 mm for the field represented in Fig. 2f). At the same time, the Rayleigh length constitutes about 5 mm at the reflected beam diameter of about 16 μm, so that to ensure efficient focusing, it is desirable to have a larger diameter of the reflected beam and, hence, of the probe beam, since the diameters of reflected and probe beams are of the same order (Figs 2d–2f). Under the condition of ideal focusing of the reflected pulse into a spot, the size of which has the order of the pulse wavelength, the pulse amplitude may reach highly relativistic values (for the frequency corresponding to the X-ray pulse frequency); if the focusing is less efficient, one can obtain a pulse possessing a relativistic intensity and a duration of a few dozen attoseconds.

4. Discussion of the results and conclusions

The scheme of generating coherent attosecond X-ray pulses, which employs reflection of the counter-propagating high-amplitude laser pulses from relativistic electron mirrors located in the accelerating pulse field requires the use of a target consisting of a single-layer nanofilm, in contrast to the scheme that uses a two-layer target [14], which is its unquestionable advantage. The formation of two counter laser beams from femtosecond pulses intersecting at a certain point in space does not cause any experimental difficulties. The required power of a laser installation, depending on the planned diameter of the relativistic electron mirror, may range from hundred terawatts to several petawatts, which is also available. Thus, the main obstacle to experimental implementation of the above-discussed scheme is the need for application of non-adiabatic accelerating pulses with a sufficiently sharp front, which ensures the formation of a relativistic electron mirror with desired characteristics.

Thus, in this work we have investigated the reflection of the high-amplitude probe laser pulses from the relativistic electron mirrors located in the accelerating field of the laser pulse. By means of 2D numerical simulation, it is shown that provided the counterpropagating pulse amplitude is several times greater than the amplitude of the accelerating laser pulse, the reflection process is highly nonlinear, which is associated with destruction of the relativistic electron mirror by the counterpropagating probe pulse. This causes a significant change in the shape of the reflected X-ray pulse and its shortening up to generation of the quasi-unipolar pulses or the single-cycle pulses. The duration of such pulses may constitute 50–60 as at the sub-relativistic amplitudes. In addition, a large amplitude of the probe pulse leads to the emergence of a large curvature of the relativistic electron mirror, which, in principle, allows us to obtain, as a result of focusing, a relativistic-intensity pulse with a duration of several dozen attoseconds. By varying the probe pulse amplitude, it is possible to control the position of the focal point of the reflected X-ray pulse.

Acknowledgements. The work was supported by the Russian Science Foundation (Project No. №14-12-01259).

References

1. Einstein A. *Ann. Phys. (Leipzig)*, **322**, 891 (1905).
2. Kulagin V.V., Cherepenin V.A., Hur M.S., et al. *Phys. Rev. Lett.*, **99**, 124801 (2007).
3. Kulagin V.V., Cherepenin V.A., Gulyaev Y.V., et al. *Phys. Rev. E*, **80**, 016404 (2009).
4. Bulanov S.V., Esirkepov T.Zh., Tajima T. *Phys. Rev. Lett.*, **91**, 085001 (2003).
5. Esirkepov T.Zh., Bulanov S.V., Kando M., et al. *Phys. Rev. Lett.*, **103**, 025002 (2009).
6. Kulagin V.V., Cherepenin V.A., Suk H. *Appl. Phys. Lett.*, **85**, 3322 (2004).
7. Cherepenin V.A., Kulagin V.V. *Phys. Lett. A*, **321**, 103 (2004).
8. Kulagin V.V., Cherepenin V.A., Suk H. *Phys. Plasmas*, **11**, 5239 (2004).
9. Habs D., Hegelich M., Schreiber J., et al. *Appl. Phys. B*, **93**, 349 (2008).
10. Wu H.-C., Meyer-ter-Vehn J. *Eur. Phys. J. D*, **55**, 443 (2009).
11. Qiao B., Zepf M., Borghesi M., et al. *New J. Phys.*, **11**, 103042 (2009).
12. Wu H.-C., Meyer-ter-Vehn J., Fernandez J., Hegelich B.M. *Phys. Rev. Lett.*, **104**, 234801 (2010).
13. Wu H.-C., Meyer-ter-Vehn J., Hegelich B.M., et al. *Phys. Rev. Spec. Top. Accel. Beams*, **14**, 070702 (2011).
14. Wu H.-C., Meyer-ter-Vehn J. *Nat. Photonics*, **6**, 304 (2012).
15. Kulagin V.V., Kornienko V.N., Cherepenin V.A., Suk H. *Kvantovaya Elektron.*, **43**, 443 (2013) [*Quantum Electron.*, **43**, 443 (2013)].
16. Kiefer D., Henig A., Jung D., et al. *Eur. Phys. J. D*, **55**, 427 (2009).
17. Paz A., Kuschel S., Rodel C., et al. *New J. Phys.*, **14**, 093018 (2012).
18. Kiefer D., Yeung M., Dzelzainis T., et al. *Nat. Commun.*, **4**, 1763 (2013).
19. McComas D.J., Allegrini F., Pollock C.J., et al. *Rev. Sci. Instrum.*, **75**, 4863 (2004).
20. Ma W., Liechtenstein V.Kh., Szerypo J., et al. *Nucl. Instrum. Methods A*, **655**, 53 (2011).

21. Bai J., Zhong X., Jiang S., et al. *Nat. Nanotechnol*., **5**, 190 (2010).
22. Henig A., Steinke S., Schnurer M., et al. *Phys. Rev. Lett*., **103**, 045002 (2009).
23. Bulanov S.V. *IEEE Trans. Plasma Sci.*, **24**, 393 (1996).
24. Vshivkov V.A., Naumova N.M., Pegoraro F., Bulanov S.V. *Phys. Plasmas*, **5**, 2727 (1998).
25. Kulagin V.V., Cherepenin V.A., Hur M.S., Suk H. *Phys. Plasmas*, **11**, 113102 (2007).
26. Nam I.H., Kulagin V.V., Hur M.S., et al. *Phys. Rev. E*, **85**, 026405 (2012).